Report

Visual Crowding at a Distance during Predictive Remapping

William J. Harrison,[1,3,*] James D. Retell,[1]
Roger W. Remington,[1] and Jason B. Mattingley[1,2]
[1]School of Psychology
[2]Queensland Brain Institute
The University of Queensland, St. Lucia, QLD 4072, Australia

Summary

When we move our eyes, images of objects are displaced on the retina, yet the visual world appears stable. Oculomotor activity just prior to an eye movement contributes to perceptual stability by providing information about the predicted location of a relevant object on the retina following a saccade [1, 2]. It remains unclear, however, whether an object's features are represented at the remapped location. Here, we exploited the phenomenon of visual crowding [3] to show that presaccadic remapping preserves the elementary features of objects at their predicted postsaccadic locations. Observers executed an eye movement and identified a letter probe flashed just before the saccade. Flanking stimuli were flashed around the location that would be occupied by the probe immediately following the saccade. Despite being positioned in the opposite visual field to the probe, these flankers disrupted observers' ability to identify the probe. Crucially, this "remapped crowding" interference was stronger when the flankers were visually similar to the probe than when the flanker and probe stimuli were distinct. Our findings suggest that visual processing at remapped locations is featurally dependent, providing a mechanism for achieving perceptual continuity of objects across saccades.

Results

Experiment 1: Remapped Crowding

Each time we make an eye movement, the retinal image is displaced, yet our perception of the visual world remains stable. The visual system achieves perceptual stability by using the magnitude and direction of an impending saccade to predictively update an internal representation of the visual world. Neurons in primate oculomotor areas, including the lateral intraparietal area (LIP), frontal eye fields (FEF), and superior colliculus (SC), begin to respond to visual stimuli outside their receptive fields if an impending saccade will bring the stimulus into the receptive field [1, 4–6]. Such anticipatory activity might provide a neural mechanism for predictive remapping of stimuli to facilitate transsaccadic perception [7]. However, whether presaccadic activity of remapping neurons conveys information about an object's identity, such as its orientation and shape, has been the subject of intense debate [8–19]. Here we demonstrate that visual processing at predictively

remapped locations is contingent on the visual appearance of the remapped object.

We exploited the phenomenon of visual crowding [3, 20] to determine whether processing at remapped locations is sensitive to features of the remapped object (see Figure 1A). A crowded object is difficult to identify because its features are integrated with those of the flanking elements prior to recognition [21]. Flankers that share features with a crowded object impair identification of the object more than flankers with nonshared features [22], and the magnitude of crowding decreases as the flankers are moved further away [3]. Crucially, in the current study, we presented a probe stimulus in one visual hemifield and distractors in the opposite visual hemifield flanking the predicted postsaccadic retinotopic location of the probe (Figure 1B). We further manipulated the similarity of flankers and probes to determine whether featural similarity modulated interference by distractors at the probe's future retinotopic location during the period of predictive remapping (Figure 1C; and see Figures S1C and S1D available online).

After first establishing a standard crowding effect (Figure S1A), we compared observers' accuracy for displays in which probe and flanker items shared visual features with their accuracy for displays in which probe and flanker features were different. As expected [22], letter probes were released from crowding when nonshared-feature flankers surrounded the probe. Specifically, probe identification accuracy was lower when flankers and probes shared features (0.50 ± 0.03; mean $\pm$ SEM; red dashed lines in Figure 2B) than when they did not (0.74 ± 0.02; blue dashed lines in Figure 2B; $t_4 = 11.56$, $p = 3.18 \times 10^{-4}$).

To measure visual processing during remapping, we required observers to identify a letter probe flashed briefly in the interval immediately prior to execution of a goal-directed saccade to a predictable location (see Figure 1C). The probe appeared in one of four possible flanker conditions: (1) directly flanked by distractors that shared features with the probe ("shared-feature" distractors); (2) directly flanked by distractors that were featurally distinct from the probe ("nonshared-feature" distractors); (3) alone in one hemifield, with shared-feature distractors presented in the opposite hemifield; or (4) alone in one hemifield, with nonshared-feature distractors presented in the opposite hemifield.

Predictive remapping is highly dependent on the time course of stimulus presentation relative to saccade onset [1, 2, 23, 24]. To motivate observers to execute saccades with predictable latencies, therefore, we required observers to report the identity of a brief, masked Gabor at the saccade target in addition to the letter probe (see Supplemental Experimental Procedures). Results from the saccade task are presented in Figure S2.

For critical "remapped crowding" trials (Figure 2A), we compared the accuracy of probe identification when no saccade was planned with accuracy during a brief period just prior to a saccade. As shown in Figure 2B, relative to no-saccade trials, probe performance was significantly reduced during the presaccade interval when both shared-feature flankers ($t_4 = 6.24$, $p = 0.003$) and nonshared-feature flankers ($t_4 = 3.13$, $p = 0.035$) surrounded the remapped location of the probe.

[3]Present address: Schepens Eye Research Institute, Massachusetts Eye and Ear Infirmary, Department of Ophthalmology, Harvard Medical School, Boston, MA 02114, USA
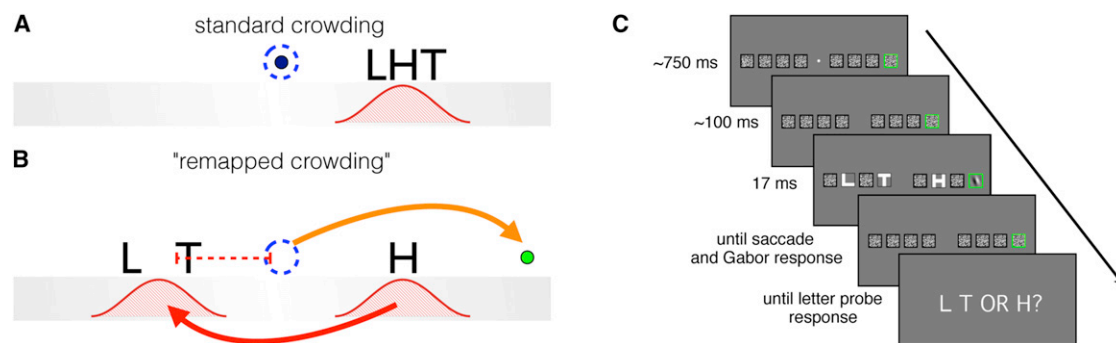*Correspondence: willjharri@gmail.com

Figure 1. Using Visual Crowding to Test Predictive Remapping

(A) Standard crowding. While fixating the blue spot in the top row, an observer would find it difficult to identify the letter H in the right visual field because of crowding, whereas identifying the letter H in (B) is relatively simple.

(B) Hypothesized "remapped crowding." If an impending saccade (orange arrow) will displace the retinal position of the H to a predicted location (dashed red line), the focus of visual processing will be remapped (red arrow) during the presaccadic interval. If predictive remapping preserves an object's features, the visual system will begin processing features matching those of the H at the remapped location in anticipation of those features appearing there after the saccade. Thus, during predictive remapping, the identity of a letter probe in the *right* hemifield should be degraded by flankers at the predicted postsaccadic location in the *left* hemifield. Gaussian distributions represent hypothetical neural activity at positions in visual cortex supporting object recognition.

(C) Display sequence from a critical trial in experiment 1, in which we tested for "remapped crowding." Probes and flankers were presented around the period of saccadic remapping. At the offset of a central fixation point (white spot), observers were required to execute a horizontal saccade to the saccade target (outlined in green on every trial) and to report the orientation of the Gabor at this location. Observers reported which letter (L, T, or H) had appeared in the placeholder located midway between fixation and the saccade target (in the diagram, the third placeholder from the right).

See also Figure S1.

These results indicate that an object's identity can be degraded by flankers in the contralateral visual field due to predictive remapping. We refer to this presaccadic perceptual effect as "remapped crowding."

A second important finding shown in Figure 2B is that remapped crowding was significantly stronger in the shared-feature condition than in the nonshared-feature condition, suggesting that, as in normal crowding, visual processing at remapped locations is sensitive to feature information. This difference was confirmed by a significant interaction between flanker features (nonshared versus shared) and saccadic condition (no saccade versus presaccade; $F_{1,4}$ = 30.51, p = 0.005). Whereas, in the no-saccade condition, probe performance was equivalent across flanker features (t_4 = 0.8, p = 0.471), in the presaccade condition, performance deteriorated more when flankers shared features with the probe than when they were featurally distinct (t_4 = 6.01, p = 0.004).

We examined the time course of interference from remapped crowding by dividing the presaccade interval into 100 ms bins measured from saccade onset (see Supplemental Experimental Procedures and Figures S1C and S1D). As shown in Figure 2C, the difference in probe identification accuracy for shared-feature and nonshared-feature conditions emerged 100–200 ms prior to saccade onset (t_4 = 3.82, p = 0.019) and was greatest 0–100 ms before the saccade (t_4 = 3.75, p = 0.020).

The results of experiment 1 demonstrate that, just prior to a goal-directed eye movement, identification of a letter probe is degraded when flankers surround the remapped location of the probe, even though at the time of presentation they appear in opposite hemifields. This remapped crowding effect is greater when flankers share features with the probe than when they are featurally distinct. Our evidence supports the conclusion that predictive remapping leads to crowding at a distance, arising from integration of feature information from the flankers and the remapped object in the opposite visual field.

Experiment 2: The Extent of Feature Specificity in Remapped Crowding

In experiment 1 the probe and shared-feature flankers were drawn from the same set of letters (L, T, and H) from trial to trial. It is possible, therefore, that at least some of the errors in probe identification might have arisen from decision noise associated with selecting between these possible letter identities [25, 26]. We ruled out this potential contribution in experiment 2 by employing shared-feature flankers, Landoldt Cs, that were never probes (see Figure 3A).

As expected [22, 27], when probes were directly flanked by distractors, the standard crowding effect was significantly stronger in the shared-feature condition than in the nonshared-feature condition (t_4 = 5.49, p = 0.005; dashed lines in Figure 3B). These results demonstrate a standard crowding effect from elementary features of flankers and probes in the absence of shared categorical identities.

As shown in Figure 3B, when the probe and flankers appeared in opposite visual hemifields, probe performance was lower during the presaccade interval of saccade trials than during fixation trials. Crucially, however, this decrement in accuracy for saccade trials was significant in the shared-feature condition (t_4 = 4.29, p = 0.013), but not in the nonshared-feature condition (t_4 = 2.02, p = 0.114). Moreover, an analysis of trials in which the probe was presented during the critical period of remapping (0–100 ms prior to the saccade) revealed a significant interaction between flanker features and saccade condition ($F_{1,4}$ = 8.39, p = 0.044). No effect of flanker similarity was observed in no-saccade conditions (t_4 = 0.31, p = 0.772). In contrast, accuracy was significantly lower during the period of predictive remapping when flankers surrounding the remapped location shared features with the probe than when the flankers were featurally distinct (t_4 = 2.82, p = 0.048; see Figure 3C). The size of this decrement was 9%, comparable to the 10% difference found for similar and distinct flankers under our standard crowding condition.
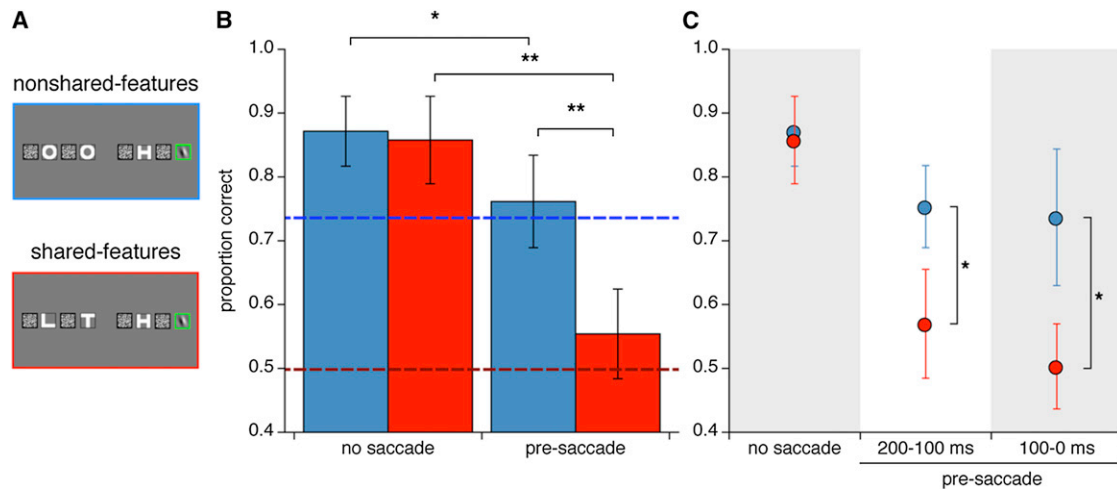
Figure 2. Feature Processing during Predictive Remapping

(A) The two critical displays used to test whether visual processing during remapping is influenced by featural information.

(B) The proportion of letters correctly identified when probes and flankers appeared in no-saccade trials and in the presaccade interval of saccade trials. Red and blue bars represent accuracy for shared-feature and nonshared-feature conditions, respectively. Dark red and dark blue dashed lines represent accuracy for standard crowding conditions with shared-feature or nonshared-feature flankers, respectively.

(C) Presaccade probe identification, plotted as a function of time prior to saccade onset (shown in separate 100 ms time bins). Error bars represent one SEM. n = 5; *p < 0.05, **p < 0.01.

See also Figure S2.

Although observers' accuracy at identifying the orientation of the Gabor differed across conditions, further analyses suggest it is unlikely these differences contributed to the remapped crowding effect (see Figure S3). Furthermore, there were no differences in saccadic latencies or amplitudes across conditions.

Experiment 3: The Spatial Extent of Remapped Crowding

Flankers degrade object recognition most strongly when they fall within an area that is approximately half the eccentricity of the probe [20], a region referred to as the "critical distance of crowding" [3]. To examine the spatial extent of feature processing at remapped locations, in experiment 3 we varied the distance of the flankers from the remapped location of the probe. Flankers were either inside (1.3°) or outside (2.6°) the critical distance of the probe's remapped location (see Figure 4A). If remapped crowding depends on the remapped location of the probe, observers' performance should be worse when flankers are 1.3° from the probe's remapped location than when they are 2.6° from the probe's remapped location.

During steady fixation and when flankers and probe appeared in the same hemifield, observers were less accurate in identifying the probe in the 1.3° flanker condition than in the 2.6° flanker condition (t_9 = 2.11, p = 0.064; see dashed lines in Figure 4B). A similar trend was observed during the presaccade interval (t_9 = 2.03, p = 0.073). These trends accord well with previous results on the effect of probe-flanker distance in crowding (for a review, see [3]). Results from the saccade task are presented in Figure S4.

As can be seen in Figure 4B, when flankers surrounded the probe's remapped location, probe identification accuracy was lower during the presaccade interval than during steady fixation in both the 2.6° condition (t_9 = 2.47, p = 0.032) and the 1.3° condition (t_9 = 4.48, p = 0.002). Note that probe identification accuracies in the no-saccade conditions were lower than those in the previous experiments. The probe was likely harder to identify in this experiment due to its greater eccentricity of 3.9° compared with 2.6° in the last experiments. Critically, as shown in Figure 4C, the time course of the presaccadic decrement was markedly different across the two spatial separations. At 0–100 ms prior to the saccade, there was an interaction between flanker spacing and saccade condition ($F_{1,9}$ = 5.57, p = 0.043): probe identification was significantly poorer for the 1.3° flanker condition than for the 2.6° flanker condition during predictive remapping (t_9 = 2.78, p = 0.021), but there was no such difference in the no-saccade condition (t_9 = 0.14, p = 0.888). Just as recognition of a visual object in the periphery depends on the proximity of surrounding objects [20], remapped crowding depends on the proximity of visual information to the remapped location of the probe.

Discussion

We found that, just prior to a saccade, the presence of visual distractors surrounding a probe letter's predicted postsaccadic retinotopic location interferes with observers' ability to identify the probe. Importantly, this interference is modulated by the visual similarity of the distractors and the probe, as in standard crowding: flankers that are similar to a probe impair performance relative to flankers that are dissimilar to a probe. In a further experiment, we also observed remapped crowding for vertical saccades, suggesting the effect is not unique to the horizontal meridian (see Supplemental Results). Our results reveal that visual features are preserved during remapping. We describe this effect as a "preservation" of visual features, rather than as "feature remapping" per se, because our data do not distinguish between competing accounts of the underlying mechanisms. Instead, our findings call attention to a fundamental regularity in the effects of remapping: just prior to saccade initiation, visual processing at the future retinotopic location of a task-relevant visual object is tuned to the features that most closely match the object.
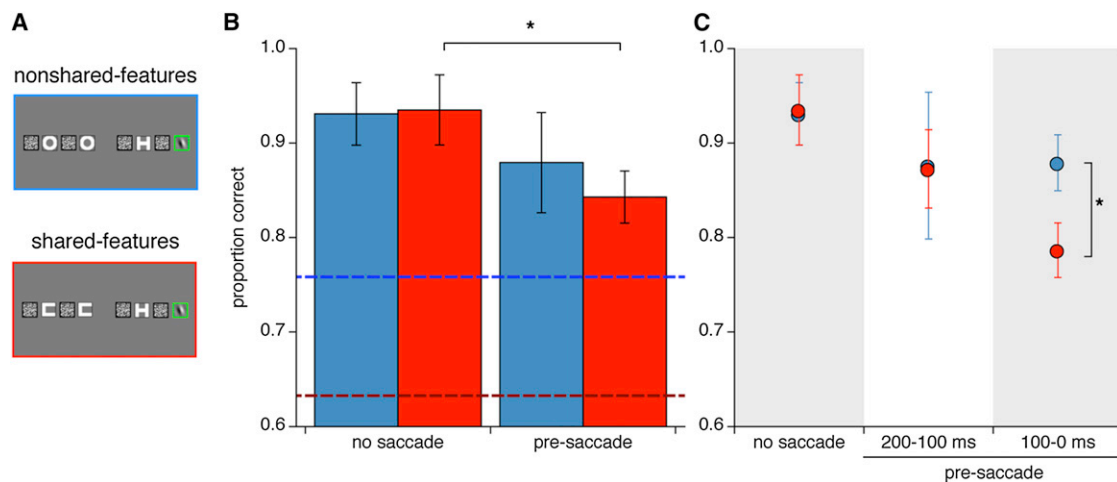
Figure 3. Remapped Crowding Depends on the Features of Flankers, Not Their Identities

(A) The shared-feature (red frame) and nonshared-feature (blue frame) displays were matched such that flankers could never be probes.

(B) The reduction in probe identification accuracy during the presaccade interval was significant only when flankers shared features with the probe.

(C) There was a significant difference in remapped crowding between shared-feature and nonshared-feature conditions, arising 0–100 ms prior to the onset of the saccade. This difference is similar in size to the difference in standard crowding shared-feature (dark red dashed line in B) and nonshared-feature conditions (dark blue dashed line in B). Error bars represent one SEM. n = 5; *p < 0.05.

See also Figure S3.

The temporal profile of the remapped crowding effect measured here closely matches the time course of activity of remapping neurons in LIP [1], area V3 [5], FEF [6, 28], and SC [4], as well as predictive remapping of spatial attention [2, 23, 24]. Hunt and Cavanagh [23] found a similar time course of interference from masks presented at the future retinotopic location of probes. They attributed this "remapped masking" effect to a shift in the priority of visual processing from the probe location to the mask location just prior to an eye movement. Because masking depends on disruption of transient signals, however, no strong conclusions could be drawn about

featural information at the remapped location. Our finding that remapped crowding depends on the similarity between flanker and probe stimuli makes remapped crowding distinct from transsaccadic [29] and presaccadic [23] remapped backward masking.

The spatial characteristics of remapped crowding are markedly different from those of standard crowding. In standard crowding, the probe and flankers appear in close spatial proximity [20]. By contrast, in remapped crowding, the flankers appear in the opposite visual hemifield to the probe. Given this difference between the physical arrangements of stimuli,
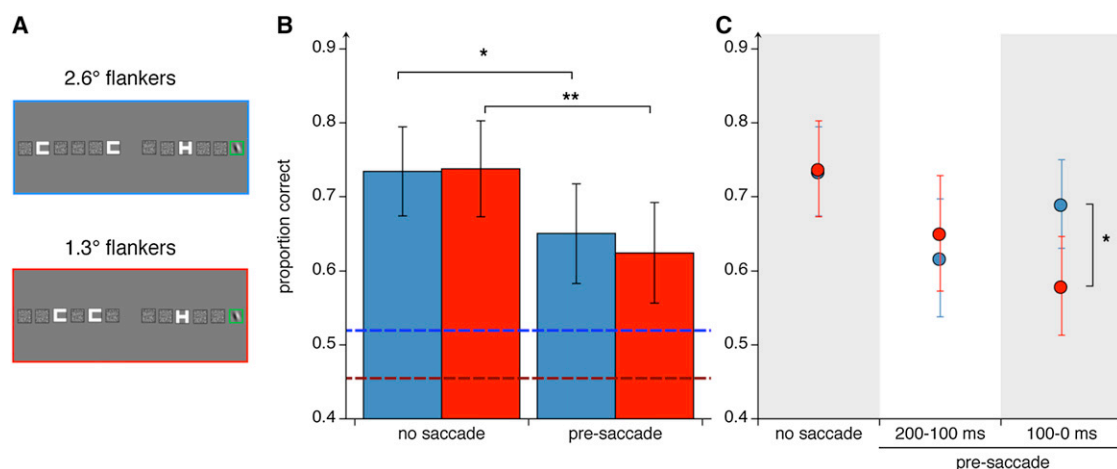

Figure 4. Remapped Crowding Depends on the Distance of Flankers from the Probe's Remapped Location

(A) Flankers appeared beyond the critical distance of the remapped location of the probe (blue frame) or within the critical distance of the remapped location of the probe (red frame).

(B) Probe identification accuracy diminished during the presaccade interval at both flanker eccentricities.

(C) Within 100 ms of a saccade, performance was significantly worse in the 1.3° flanker condition than in the 2.6° flanker condition. This difference is similar in size to the difference in standard crowding with flankers at 1.3° from the probe (dark red dashed line in B) versus 2.6° from the probe (dark blue dashed line in B). Error bars represent one SEM. n = 10; *p < 0.05, **p < 0.01.

See also Figure S4.

the analogous reduction in identification accuracy in the standard and remapped conditions is most likely attributable to a common form of spatiotemporal integration of probe and flanker stimuli (see the Supplementary Material of [3]). During predictive remapping, there is a brief window of time during which visual processing is prioritized at the location of the probe and, concurrently, at its predicted location [2]. On this account, remapped crowding arises because visual information is drawn from both the probe and the flankers, resulting in visual interference. Such an interpretation is in line with evidence from a recent study, in which we found that oculomotor signals play an important role in visual crowding [30], and is consistent with the notion that feature preservation during remapping is mediated by higher brain areas, such as FEF [15].

A link between an object's position and identity could be mediated in a top-down fashion by brain areas involved in both remapping and visual selection, potentially negating the need for feature information to be conveyed via the remapping signal itself [7, 15]. The FEF, for example, contain remapping neurons [6] and specify the locations of visual objects with task-relevant features [31]. Thus, just prior to a saccade, neurons in such remapping areas can signal the remapped position of an object with task-relevant features. Reciprocal links between FEF and area V4 allow dynamic, spatiotemporal changes in featural processing [32] at remapped locations [15]. Top-down mediation of feature preservation during remapping provides a mechanism by which transsaccadic object continuity could be achieved via purely retinotopic representations [11–13, 15], without the need to transfer feature gain settings of low-level visual neurons, as previously suggested [10, 33]. Our account is in line with recent studies showing that the degree of postsaccadic remapping can be modulated by instructing observers to attend to the remapped location of objects [34–36] (but see [13]), as well as a recent brain imaging study showing that a world-referenced representation of motion depends on the allocation of spatial attention to the motion stimulus [37].

We have shown that, during eye movement preparation, visual processing is altered to anticipate the appearance of task-relevant features at the predicted postsaccadic location of a visual object. Under natural conditions, top-down preservation of features during remapping would allow an uninterrupted and stable representation of visual objects across shifts of gaze, because relevant object features are primed at remapped locations in expectation of these features arriving there following an eye movement.

Supplemental Information

Supplemental Information includes four figures, Supplemental Results, and Supplemental Experimental Procedures and can be found with this article online at http://dx.doi.org/10.1016/j.cub.2013.03.050.

References

1. Duhamel, J.R., Colby, C.L., and Goldberg, M.E. (1992). The updating of the representation of visual space in parietal cortex by intended eye movements. Science *255*, 90–92.

2. Rolfs, M., Jonikaitis, D., Deubel, H., and Cavanagh, P. (2011). Predictive remapping of attention across eye movements. Nat. Neurosci. *14*, 252–256.

3. Pelli, D.G., and Tillman, K.A. (2008). The uncrowded window of object recognition. Nat. Neurosci. *11*, 1129–1135.

4. Walker, M.F., Fitzgibbon, E.J., and Goldberg, M.E. (1995). Neurons in the monkey superior colliculus predict the visual result of impending saccadic eye movements. J. Neurophysiol. *73*, 1988–2003.

5. Nakamura, K., and Colby, C.L. (2002). Updating of the visual representation in monkey striate and extrastriate cortex during saccades. Proc. Natl. Acad. Sci. USA *99*, 4026–4031.

6. Sommer, M.A., and Wurtz, R.H. (2006). Influence of the thalamus on spatial visual processing in frontal cortex. Nature *444*, 374–377.

7. Wurtz, R.H. (2008). Neuronal mechanisms of visual stability. Vision Res. *48*, 2070–2089.

8. Melcher, D., and Morrone, M.C. (2003). Spatiotopic temporal integration of visual motion across saccadic eye movements. Nat. Neurosci. *6*, 877–881.

9. Melcher, D. (2005). Spatiotopic transfer of visual-form adaptation across saccadic eye movements. Curr. Biol. *15*, 1745–1748.

10. Melcher, D. (2007). Predictive remapping of visual features precedes saccadic eye movements. Nat. Neurosci. *10*, 903–907.

11. Knapen, T., Rolfs, M., and Cavanagh, P. (2009). The reference frame of the motion aftereffect is retinotopic. J. Vis. *9*, 16.1-7.

12. Afraz, A., and Cavanagh, P. (2009). The gender-specific face aftereffect is based in retinotopic not spatiotopic coordinates across several natural image transformations. J. Vis. *9*, 10.1-17.

13. Knapen, T., Rolfs, M., Wexler, M., and Cavanagh, P. (2010). The reference frame of the tilt aftereffect. J. Vis. *10*, 8.1-13.

14. Morris, A.P., Liu, C.C., Cropper, S.J., Forte, J.D., Krekelberg, B., and Mattingley, J.B. (2010). Summation of visual motion across eye movements reflects a nonspatial decision mechanism. J. Neurosci. *30*, 9821–9830.

15. Cavanagh, P., Hunt, A.R., Afraz, A., and Rolfs, M. (2010). Visual stability based on remapping of attention pointers. Trends Cogn. Sci. *14*, 147–153.

16. Melcher, D. (2010). The missing link for attention pointers: comment on Cavanagh et al. Trends Cogn. Sci. *14*, 473.

17. Cavanagh, P., Hunt, A.R., Afraz, A., and Rolfs, M. (2010). Attentional pointers: response to Melcher. Trends Cogn. Sci. *14*, 474–475.

18. Mayo, J.P., and Sommer, M.A. (2010). Shifting attention to neurons. Trends Cogn. Sci. *14*, 389.

19. Cavanagh, P., Hunt, A.R., Afraz, A., and Rolfs, M. (2010). Attention Pointers: Response to Mayo and Sommer. Trends Cogn. Sci. *14*, 390–391.

20. Bouma, H. (1970). Interaction effects in parafoveal letter recognition. Nature *226*, 177–178.

21. Levi, D.M. (2008). Crowding—an essential bottleneck for object recognition: a mini-review. Vision Res. *48*, 635–654.

22. Kooi, F.L., Toet, A., Tripathy, S.P., and Levi, D.M. (1994). The effect of similarity and duration on spatial interaction in peripheral vision. Spat. Vis. *8*, 255–279.

23. Hunt, A.R., and Cavanagh, P. (2011). Remapped visual masking. J. Vis. *11*, 13.

24. Jonikaitis, D., Szinte, M., Rolfs, M., and Cavanagh, P. (2013). Allocation of attention across saccades. J. Neurophysiol. *109*, 1425–1434.

25. Chastain, G. (1982). Confusability and interference between members of parafoveal letter pairs. Percept. Psychophys. *32*, 576–580.

26. Gervais, M.J., Harvey, L.O., Jr., and Roberts, J.O. (1984). Identification confusions among letters of the alphabet. J. Exp. Psychol. Hum. Percept. Perform. *10*, 655–666.

27. Parkes, L., Lund, J., Angelucci, A., Solomon, J.A., and Morgan, M. (2001). Compulsory averaging of crowded orientation signals in human vision. Nat. Neurosci. *4*, 739–744.

28. Umeno, M.M., and Goldberg, M.E. (1997). Spatial processing in the monkey frontal eye field. I. Predictive visual responses. J. Neurophysiol. *78*, 1373–1383.

29. De Pisapia, N., Kaunitz, L., and Melcher, D. (2010). Backward masking and unmasking across saccadic eye movements. Curr. Biol. *20*, 613–617.

30. Harrison, W.J., Mattingley, J.B., and Remington, R.W. (2013). Eye movement targets are released from visual crowding. J. Neurosci. *33*, 2927–2933.

31. Schall, J.D. (2002). The neural selection and control of saccades by the frontal eye field. Philos. Trans. R. Soc. Lond. B Biol. Sci. *357*, 1073–1082.

32. Moore, T., and Armstrong, K.M. (2003). Selective gating of visual signals by microstimulation of frontal cortex. Nature *421*, 370–373.

33. Melcher, D., and Colby, C.L. (2008). Trans-saccadic perception. Trends Cogn. Sci. *12*, 466–473.

34. Melcher, D. (2009). Selective attention and the active remapping of object features in trans-saccadic perception. Vision Res. *49*, 1249–1255.

35. Golomb, J.D., Chun, M.M., and Mazer, J.A. (2008). The native coordinate system of spatial attention is retinotopic. J. Neurosci. *28*, 10654–10662.

36. Golomb, J.D., Nguyen-Phuc, A.Y., Mazer, J.A., McCarthy, G., and Chun, M.M. (2010). Attentional facilitation throughout human visual cortex lingers in retinotopic coordinates after eye movements. J. Neurosci. *30*, 10493–10506.

37. Crespi, S., Biagi, L., d'Avossa, G., Burr, D.C., Tosetti, M., and Morrone, M.C. (2011). Spatiotopic coding of BOLD signal in human visual cortex depends on spatial attention. PLoS ONE *6*, e21661.

Visual Crowding at a Distance
during Predictive Remapping

William J. Harrison, James D. Retell, Roger W. Remington, and Jason B. Mattingley

Supplemental Inventory

Supplemental Figures
Figure S1 shows data from a pilot experiment in which we established standard crowding and remapped crowding effects, and the timing of stimuli according to saccade onset in the main experiments. Figures S2–S4 show results from analyses of the Gabor orientation judgment task, saccadic latencies, and saccade amplitudes for the three main experiments. In Figures S2–S4, pre-saccade trials included only those in which the probe was presented within 100 ms of saccade onset, when remapped crowding was strongest in all experiments. All differences in Gabor accuracy were analysed with 2 x 2 repeated measures ANOVAs, and pairwise t-tests were used to explore any significant interactions. Saccadic latencies and saccade amplitudes were evaluated using two-tailed paired t-tests with $\alpha = 0.05$.

Supplemental Results
Here we report results from a Supplemental Experiment in which we tested for remapped crowding with vertical saccades (see Discussion in the main text).

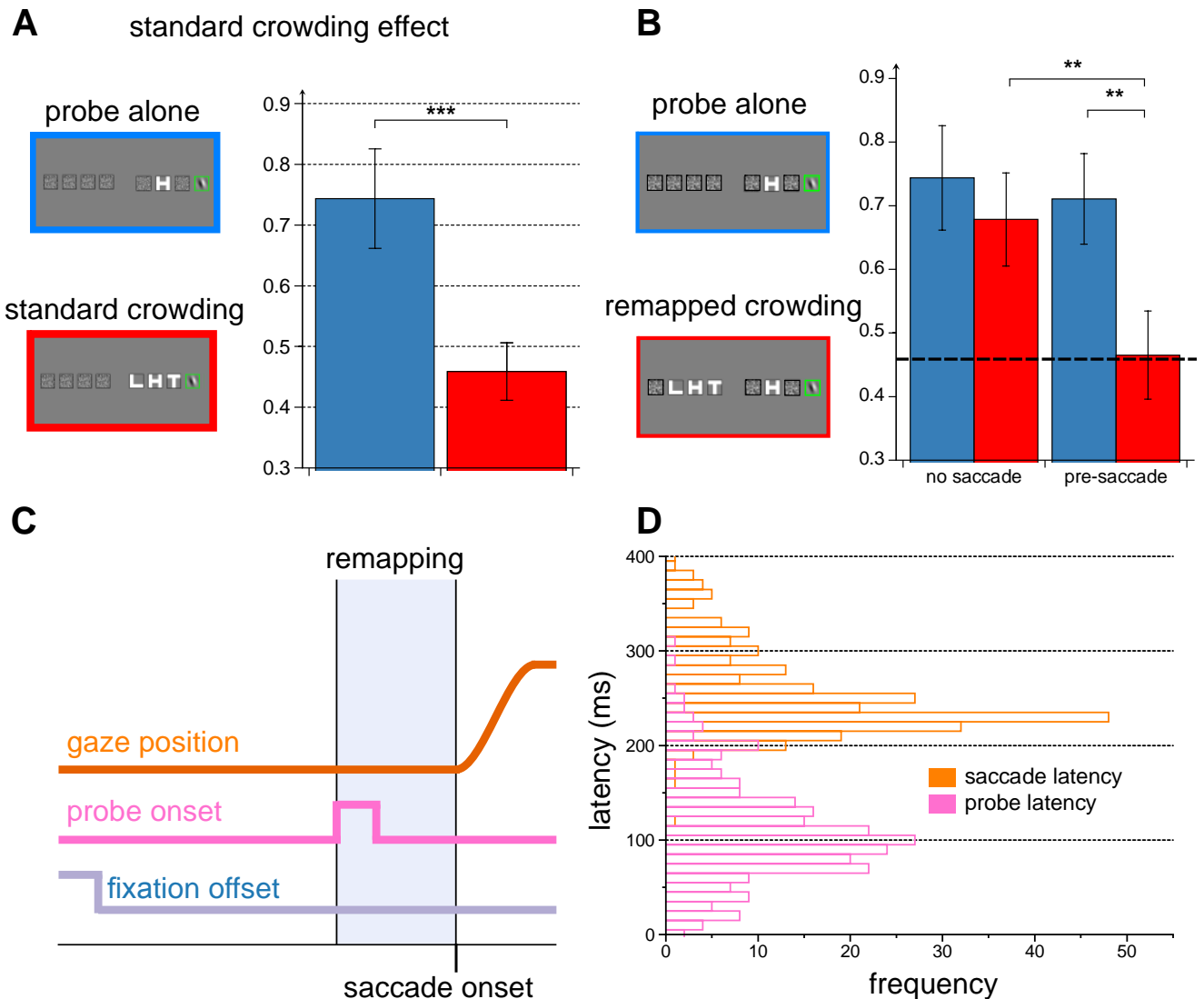**Supplemental Experimental Procedures**

Figure S1, Related to Figure 1. Standard Crowding, Remapped Crowding, and Stimulus Timing

(**A and B**) Data from a pilot experiment (N = 10). (**A**) While observers remained fixated in the center of the display, identification accuracy for a probe flanked by letters (red bar) was significantly lower than for a probe presented alone (blue bar; p = 0.004). (**B**) In the no-saccade condition, the presence of distractors in the hemifield opposite the probe had no effect on probe identification accuracy relative to probe-alone trials (p > 0.10). For trials in which an eye movement had to be executed, however, participants' accuracy in identifying probes during the pre-saccade interval was significantly reduced when distractors occupied the probe's remapped location relative to probe-alone trials. Statistical analyses confirmed a significant two-way interaction between saccade condition (no-saccade versus pre-saccade) and flanker condition (probe-alone versus remapped crowding; $F_{1,9}$ = 7.97, p = 0.02). Specifically, the difference in accuracy

between probe-alone and remapped crowding conditions was significant only during the pre-saccade interval ($t_9 = 3.58$, $p = 0.006$). Furthermore, while the decrease in accuracy from no-saccade to pre-saccade trials was significant for the remapped crowding condition ($t_9 = 3.29$, $p = 0.009$), there was no such difference for the probe alone condition ($t_9 = 0.99$, $p = 0.347$). The dashed black line shows performance for the standard crowding condition. Note that it was only in the pilot experiment that the "remapped crowding" display contained two probe letters, one in each hemifield, as shown here. Error bars in (**A**) and (**B**) represent one SEM. *** $p = 0.001$; ** $p < 0.01$.

(**C**) Overview of the timing of probe onset relative to fixation offset in critical "remapped crowding" trials, aligned to saccade onset on the x-axis.

(**D**) Saccade data from a representative observer in Experiment 1. Frequency of saccadic latency is plotted in orange. Onset asynchrony between probes and saccades is shown in pink. Probe onset latencies were normally distributed around 100 ms prior to the saccade. This method yielded an approximately equal number of observations across 100 ms time bins (see Supplemental Experimental Procedures).
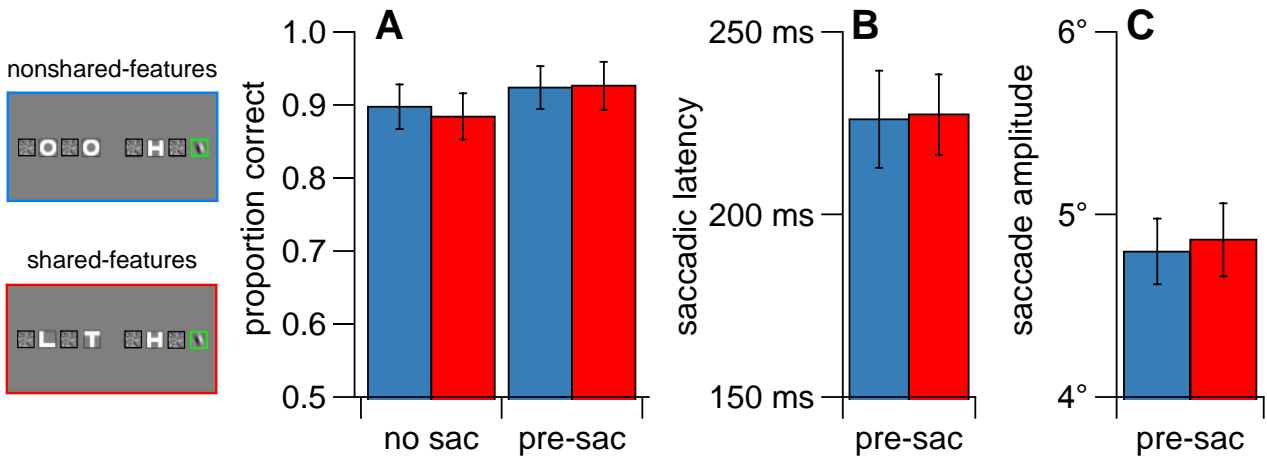
Figure S2, Related to Figure 2. Experiment 1: Gabor Judgment Accuracies, Saccadic Latencies, and Saccade Amplitudes

(**A**) Gabor judgment accuracy. There were no significant differences in Gabor judgement accuracy across conditions.

(**B**) Saccadic latencies. Saccadic latencies were equivalent for nonshared- and shared-feature conditions. This implies spatial attention was deployed to the Gabor equally across conditions.

(**C**) Saccade amplitudes. There was no difference in saccade amplitude across conditions. This implies the Gabor was equally attended across saccade and fixation trials. Error bars in all panels show one SEM.
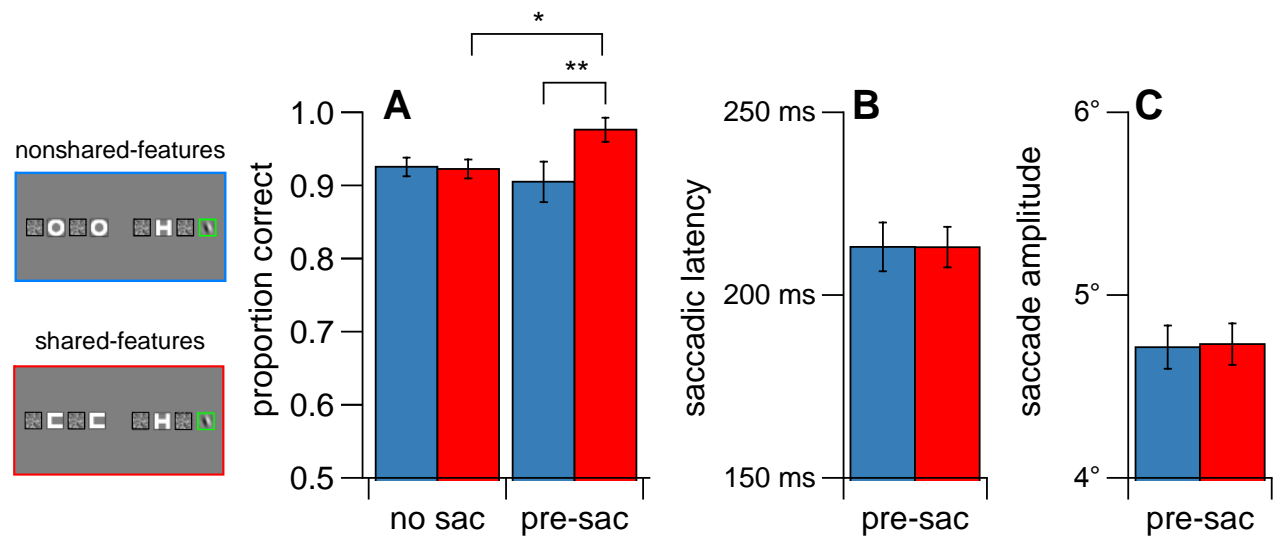
Figure S3, Related to Figure 3. Experiment 2: Gabor Judgment Accuracies, Saccadic Latencies, and Saccade Amplitudes

(**A**) Gabor judgment accuracy. We found a marginally significant interaction between flanker condition (nonshared vs shared) and saccade condition (no-saccade vs pre-saccade) for Gabor judgment accuracy ($F_{1,4} = 6.83$, $p = 0.059$). Follow-up pairwise t-tests (without correction for multiple post-hoc comparisons) revealed that, compared with fixation, observers were marginally more accurate at judging the orientation of the Gabor during the pre-saccade interval with shared-feature distractors ($t_4 = 2.33$, $p = 0.081$). Furthermore, during the pre-saccadic interval, Gabor judgments were more accurate in the shared-feature condition than in the nonshared-feature condition ($t_4 = 3$, $p = 0.04$). It may have been the case, therefore, that improved performance in the Gabor task for the shared-feature condition led to worse performance in the probe identification task during the pre-saccade interval. Indeed, we found a marginally significant correlation between improvement in Gabor accuracy and reduction in probe identification accuracy in the shared-feature condition ($r = 0.82$, $p = 0.089$). However, Gabor judgment accuracy was not causally related to probe identification accuracy: there was no such correlation for the nonshared-feature condition ($r = -0.21$, $p = 0.73$); nor was this correlation present in the shared-feature condition of either of the other main experiments (Experiment 1: $r = -0.46$, $p = 0.439$; Experiment 3: $r = -0.18$, $p = 0.623$).

(**B**) Saccadic latencies. Saccadic latencies were equivalent in the two remapped crowding conditions.

(**C**) Saccade amplitudes. There was no difference in saccade amplitude across conditions. Error bars in all panels show one SEM. * $p < 0.1$, ** $p < 0.05$.
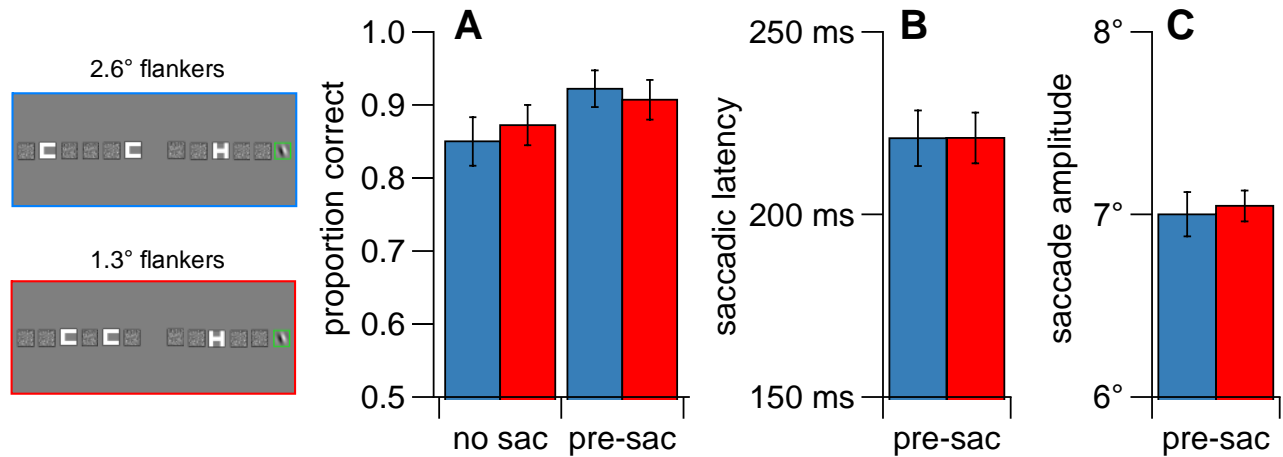
Figure S4, Related to Figure 4. Experiment 3: Gabor Judgment Accuracies, Saccadic Latencies, and Saccade Amplitudes

(**A**) Gabor judgment accuracy. There was a main effect of saccade condition (no-saccade vs pre-saccade) on Gabor judgement accuracy ($F_{1,9}$ = 8.97, p = 0.015). Critically, however, there was no interaction between flanker condition and saccade condition.

(**B**) Saccadic latencies. Saccadic latencies were equivalent for nonshared- and shared-feature conditions.

(**C**) Saccade amplitudes. There was no difference in saccade amplitude across conditions. Error bars in all panels show one SEM.

Supplemental Results

Supplemental Experiment
To test whether the findings from Experiments 1–3 might be unique to horizontal saccades, we ran a Supplemental Experiment (N = 10) to test whether remapped crowding also occurs for vertical saccades. The critical displays used were similar to the remapped crowding display shown in Figure 4A, but were rotated 90° such that all placeholders fell on the vertical meridian. The saccade target was 7.8° from the center of the display, and the probe was 3.9° from the center of the display. Flankers only appeared within the critical distance of the probe's actual location or remapped location. All other stimulus and timing details were as per Experiment 3 (see Supplemental Experimental Procedures). When flankers surrounded the probe's remapped location, the proportions of letters correctly identified in no-saccade trials and pre-saccade trials were 0.56 ± .05 (M ± SEM) and 0.45 ± .05, respectively. That is, relative to no-saccade trials, probe performance was significantly reduced during the pre-saccade interval when flankers surrounded the probe's remapped location (p = 0.006). Thus, remapped crowding also occurs for vertical saccades and is not unique to horizontal saccades or situations in which stimuli are presented on the horizontal meridian.

Supplemental Experimental Procedures

Observers
Twelve observers (4 females, 2 authors) participated in the experiments (five observers in Experiments 1 and 2, and 12 observers in Experiment 3). All observers had normal or corrected-to-normal vision. The study was approved by The University of Queensland's School of Psychology Ethical Review Committee.

Materials
Participants sat with their head in a head and chin rest positioned 57 cm from a 22-inch widescreen Dell LCD monitor (1920 x 1200 pixels, 60 Hz) in Experiments 1 and 2, and a 20-inch Dell CRT monitor (1600 x 1200 pixels, 60 Hz) in Experiment 3. Stimulus presentation, eye movement recording and response collection were programmed using the Psychophysics Toolbox Version 3 [38, 39] and Eyelink Toolbox [40] for MATLAB (MathWorks). Eye movements were recorded at 500 Hz with an EyeLink 1000 (SR Research) infrared eye tracker, calibrated using a 5-point calibration procedure.

Stimuli and Procedure
Each trial began with the presentation of a fixation dot (width = 0.2°) at the center of a uniform gray display (31.2 cd/m^2). Four placeholders (0.9° x 0.9°) in Experiments 1 and 2, and six placeholders in Experiment 3, were positioned to the left and right of the fixation spot, along the horizontal meridian. The distance from the fixation dot to the center of the nearest placeholder, and between the centers of adjacent placeholders, was 1.3°. There was a gap of 0.4° between adjacent placeholders. All placeholders

were outlined in black with the exception of either the far left or far right placeholder, which was outlined in green to indicate the saccade goal and the location of the Gabor. The side of the saccade goal was selected with equal probability across trials and presented in a pseudorandom order. The distance from the fixation dot to the center of the saccade goal was 5.2° in Experiments 1 and 2, and 7.8° in Experiment 3. To reduce perceptual distortions of space around the time of the saccade (e.g. [41]), and to eliminate transients associated with the onset and offset of the probe and any flankers, all placeholders were filled continuously with animated white noise [2], except during the target frame (Figure 1C). White noise was randomised on each screen refresh (each pixel value was pseudorandomly and independently drawn from a normal distribution, M = 128, SD = 50).

Each trial began only if gaze was maintained within a 2° x 2° area centered around the fixation spot for 500 ms. The fixation spot disappeared after a uniformly variable delay (750-1250 ms), cueing participants to execute the saccade. The saccade target (a Gabor oriented 22.5° left or right from vertical), letter probe, and any distractors were presented in a single frame during the pre-saccade interval (see below), and were immediately followed by dynamic white noise inside each placeholder. After 500 ms of white noise, participants reported the Gabor orientation with a button press (left or right arrow). If the orientation of the Gabor was reported correctly, the text, "T L or H?" was presented; participants then made a three-alternative forced-choice judgment on the identity of the letter probe via button press (left, down, or right arrow, for T, L and H, respectively). Observers were instructed that the letter probe to be identified would always appear in the placeholder located mid-way between fixation and the saccade target (i.e., the third placeholder from the end of the array in Experiments 1 and 2, and the fourth placeholder from the end of the array in Experiment 3). During testing, no feedback was given about letter probe performance. To control for any effects of flankers on probe identification that were not specific to an impending saccade, we included blocks of trials in which observers undertook the same task but were required to maintain their gaze centrally at the offset of the fixation point.

The saccade target was always located at the extreme left or right end of the array of placeholders. Participants practiced until they could execute the required eye movement and judge the orientation of the saccade target while performing above chance on the letter probe task (see below). If participants reported the orientation of the Gabor incorrectly, they were provided with on-screen feedback and informed that the trial would be repeated at the end of the block. After responses were made and any feedback given, the next trial commenced immediately. Saccade and fixation blocks of at least 16 trials were alternated, giving a minimum of 480 trials per participant. The colour of the fixation spot changed to indicate whether the observer was required to execute a saccade (indicated in blue) or remain fixated (indicated in red).

The target frame, including the letter probe, Gabor, and any distractors, was presented for 17 ms. Letter probes, distractor letters (Experiment 1) and square Landoldt Cs (Experiments 2 and 3) were constructed from rectangles (0.9° x 0.3°) arranged to form each symbol (T, H, L, C). Oval distractors in Experiments 1 and 2 had a diameter of

0.9°, and a line width of 0.3°. In Experiment 2, Landoldt Cs were always oriented with the gap on the right to ensure their identities were as consistent over trials as the dissimilar feature distractor identities (Os). In Experiment 3, the direction of each Landoldt C was randomised from trial to trial. In all experiments, probes and distractors were white (100% contrast). Based on data from a pilot study, the Gabor (1.4 cpd, 100% contrast) was oriented 22.5° left or right off vertical. Correct identification of the saccade target required close allocation of spatial attention toward the saccade goal, and away from the letter stimuli in the remapped crowding condition [42].

The interval between the saccade cue (the offset of the fixation spot) and the target frame was adjusted so the target frame was presented during the pre-saccade interval on the majority of trials (see Figure S1B and S1C) [23]. This interval was calculated by subtracting 100 ms from the median saccadic latency. To time the target frame, saccadic latencies were calculated online as the time between the offset of the fixation spot and the moment gaze deviated from this fixation point by more than 2°. Each experiment began with a block of saccade trials, and the median saccadic latency of the first trial of the first saccade block was estimated at 200 ms. Median saccadic latencies were calculated from all preceding saccades in the current block only. Reported saccadic latencies, and those used for all analyses, were re-calculated offline using the native EyeLink saccade detection criteria. This method of timing target presentations worked well and yielded close to 50% of trials in each time bin (see below and Figure S1D). The interval between the saccade cue and target frame from the most recent saccade trial was used for the following block of no-saccade trials.

Observers completed a minimum of 60 trials per distractor condition in all experiments, collapsed across probe side (left or right). The same number of trials was completed for each condition during fixation. All participants completed at least one block of 20 trials in which all stimuli were displayed as described above, but the task was to execute a saccade and report the orientation of the Gabor only. This practice block was repeated until accuracy at the Gabor orientation task exceeded 75%. Observers also completed at least one practice block of saccade and letter identification tasks, and then an entire run of trials as practice. For the pilot experiment, participants did *not* complete an entire run of practice trials. This difference in practice likely accounts for the overall higher accuracy in "no-saccade" trials for the main experiments (e.g. Figure 2B) relative to the pilot experiment (Figure S1B). Data from practice blocks were discarded.

Data Preprocessing and Statistical Analyses
Only trials in which observers correctly identified the orientation of the Gabor were included in analyses. Trials were discarded for the following reasons: (1) no saccade was executed or the saccade endpoint was greater than 2° from the center of the saccade target in saccade trials; (2) saccadic latency was shorter than 100 ms; (3) a saccade greater than 2° was executed within 500 ms of the removal of the fixation spot on fixation trials; (4) the target frame was presented during an eye-blink. Of the remaining trials, "pre-saccade" trials were those in which the onset of the target frame preceded the saccade by more than 17 ms, and by less than 200 ms. Trials in which the target frame onset occurred outside of these periods were excluded. For Experiment 3,

data were excluded for one observer due to poor performance at identifying the orientation of the Gabor (mean accuracy = 67%), and for one observer for whom there were less than 10 observations for each of two conditions. In total, 86.3% of trials were included in Experiment 1, 88.8% in Experiment 2, and 89.3% in Experiment 3. Pre-saccade trials were binned according to their onset time relative to the saccade (see Figure S1D). Of all included pre-saccade trials meeting the above criteria, 48.1% occurred 0-100 ms prior to the saccade in Experiment 1, 51.7% occurred 0-100 ms prior to the saccade in Experiment 2, and 49.4% occurred prior to the saccade in Experiment 3.

Supplemental References
38. Brainard, D. H. (1997). The Psychophysics Toolbox. Spatial Vision 10, 433–436.
39. Pelli, D. G. (1997). The VideoToolbox software for visual psychophysics: Transforming numbers into movies. Spatial Vision 10, 437–442.
40. Cornelissen, F. W., Peters, E. M., and Palmer, J. (2002). The Eyelink Toolbox: eye tracking with MATLAB and the Psychophysics Toolbox. Behav Res Methods Instrum Comput 34, 613–617.
41. Ross, J., Morrone, M. C., and Burr, D. C. (1997). Compression of visual space before saccades. Nature 386, 598–601.
42. Deubel, H., and Schneider, W. X. (1996). Saccade target selection and object recognition: evidence for a common attentional mechanism. Vision Research 36, 1827–1837.